AGU PUBLICATIONS

[Paleoceanography and Paleoclimatology]

Supporting Information for

Deglacial heat uptake by the Southern Ocean and rapid northward redistribution via Antarctic Intermediate Water

David-Willem Poggemann[a], Dirk Nürnberg[a,*], Ed C. Hathorne[a], Martin Frank[a], Willi Rath[a], Stefan Reißig[a], André Bahr[b]

[a]GEOMAR Helmholtz Centre for Ocean Research Kiel, D-24148 Kiel, Germany

[b]Heidelberg University, Institute of Earth Science, D-69120 Heidelberg, Germany

Contents of this file

Text S1 to S7

Figures S1 to S7

Table S1

Additional Supporting Information (Files uploaded separately)

Captions for Data Set S1

Introduction

We reconstructed benthic foraminiferal Mg/Ca-based intermediate water temperatures ($IWT_{Mg/Ca}$) and intermediate water Nd isotope compositions (εNd) at sub-millennial resolution from sediment cores located at the northern tip of modern AAIW extent in the tropical W-Atlantic (850 and 1018 m water depth). Pronounced warming of AAIW in the tropical W-Atlantic during Heinrich Stadial 1 (HS1) and the Younger Dryas (YD) were induced by major AMOC perturbations resulting in a pronounced accumulation of heat in the surface Southern Ocean. We speculate that the northward ocean heat redistribution *via* AAIW effectively dampened Southern Hemisphere warming during the deglaciation and was intimately linked to the major deglacial perturbations of the AMOC.

We analyzed Mg/Ca of the endobenthic foraminiferal species *Uvigerina* spp. selected from sediment core M78/1-235-1 (11°36.53'N, 60°57.86'W; termed Core 235 in the following). The core was retrieved from the Tobago Basin (SE-Caribbean) from 852 m water depth, which is within the core of modern AAIW.

We further determined the εNd signatures of uncleaned mixed planktonic foraminifera to reconstruct changes in the mixing of the prevailing intermediate water masses. The εNd signatures were extracted from nearby sediment core M78/1-222-9 (12°1.49'N, 64°28.50'W, 1018 m; termed Core 222 in the following). Core 222 was retrieved from the southern Caribbean Sea north of Blanquilla Island and located at the lower boundary of modern AAIW.

According Data Set DS01 is uploaded to AGU’s journal submission site

Text S1.

Age model of sediment core M78/1-222-9

The age model for sediment Core 222 is based on linear interpolation between 4 AMS^{14}C dates (Table S1) and supported by oxygen isotope stratigraphy (see supporting information Fig. S1). For Core 235, we use the established age model of Core 235 (Poggemann et al., 2017), which was generated by linear interpolation between 9 AMS^{14}C dates (Fig. 2).

Text S2.

Comparison of IWT-calibrations for *Uvigerina* spp.

We note that a large number of Mg/Ca$_{Uvigerina}$ based bottom water temperature calibrations are currently available (Fig. S2), which all have their strengths and weaknesses. We finally decided to present and apply the two most reasonable calibrations based on their agreement with the present-day IWTs at the core locations, which are the linear Elderfield et al. (2010) (Mg/Ca = 1 + 0.1 T) and the exponential Martin et al. (2002) calibrations (Mg/Ca = 0.76 * exp(0.15 T)). Notably, these calibrations provide latest Holocene $IWT_{Mg/Ca}$, which match the modern IWT (~5°C) at the location of Core 235 (Fig. S2) within error. The resulting downcore amplitude reconstructions of $IWT_{Mg/Ca}$ are close to each other in the low temperature range (<5°C), while the Elderfield et al. (2010) calibration provides a larger $IWT_{Mg/Ca}$ amplitude than the exponential Martin et al. (2002) equation with higher peak $IWT_{Mg/Ca}$ (Fig. 2, S7). The amplitude of these variations are smaller by up to a factor of two than the other calibrations available (Lea et al., 2002; Elderfield et al., 2006; 2010; Bryan & Marchitto, 2008; Yu & Elderfield, 2008; Roberts et al., 2016).

Text S3.

Contamination check

The effect of foraminiferal cleaning efficiency, postdepositional contamination, and diagenetic alteration on foraminiferal Mg/Ca was checked by monitoring all samples for their Fe/Ca, Al/Ca and Mn/Ca ratios, for which contamination-indicative threshold values exist (<0.1 mmol/mol; Barker et al., 2003; Them et al., 2015), bearing in mind that these threshold values may largely depend on the sediment type the foraminiferal tests were removed from (Fig. S3). Fe/Ca, Al/Ca and Mn/Ca ratios in our foraminiferal samples are mostly below the given threshold values, but at times reach values of up to 1.2 mmol/mol, ~0.7 mmol/mol, and 0.14 mmol/mol, respectively (Fig. S3). These high contaminant values do not consistently have high foraminiferal Mg/Ca ratios. There is no significant correlation of Mg/Ca to neither Fe/Ca, Al/Ca nor Mn/Ca ($R^2 = 0.15$, $R^2 = 0.19$; $R^2 = 0.06$). The downcore records of Al/Ca, Fe/Ca, and Mn/Ca (Fig. S4) further show different temporal variations than Mg/Ca, supporting our notion that Mg/Ca is bearing an unbiased oceanographic signature. In particular, the Mn/Ca ratios of our oxidatively cleaned foraminiferal samples are so low (<0.14 mmol/mol) that the Mg contribution of a diagenetic coating would be negligible. According to Roberts et al. (2016), a Mg/Mn ratio of 0.1 mol/mol (this study: on average 0.07 mol/mol Mg/Mn within foraminiferal tests) within a diagenetic coating would account for 10^{-2} mmol/mol at maximum to foraminiferal Mg/Ca in our record, which is well within the reproducibility of our Mg/Ca analyses. In conclusion, we consider sample contamination unimportant for our Mg/Ca analyses.

The validity of the prominent Mg/Ca maxima during HS1 (in particular at 15 ka) and the YD is convincingly supported by the intermediate water temperature reconstruction of Rühlemann et al. (2004) from Tobago Basin, which is shown in Fig. S4. The Rühlemann et al. (2004) reconstruction is solely based on benthic, ice-volume corrected oxygen isotope data, which basically explains minor differences in the records.

Text S4.

Data points rejected as outliers

A small number of single Mg/Ca data points yielded extremely high/low values compared with the surrounding data, and led to unrealistically high or low $IWT_{Mg/Ca}$ values (Fig. S5). We here applied the Grubbs test and defined a total of 16 Mg/Ca data as outliers, which were then removed from the Core 235 record. These Mg/Ca outliers were on average lower or higher by ~0.8 mmol/mol than the surrounding data within 0.5 kyr time intervals. The Grubbs test (also named maximum normalized residual test or extreme student deviation test) statistically detects outliers in univariate, normally distributed data sets (Grubbs, 1950; 1969).

Text S5.

Static stability check for warmed AAIW conditions

To check the plausibility of the postulated warming of AAIW in the tropical W-Atlantic during times of AMOC perturbations, we tested if 4 - 6°C warmer AAIW and the modified vertical temperature and density profiles would contradict modern-day stratification of the water masses. To this end, we diagnosed static stability as determined by the vertical (positive downward) gradient of locally referenced potential density. A positive vertical gradient (denser waters below less dense waters) indicates a (statically) stable water column, while a negative vertical gradient (less dense waters below denser waters) indicates an unstable, non-lasting configuration**.**

In our calculation, we modified modern AAIW temperatures by +5°C, close to our deglacial IWT estimate in the tropical W-Atlantic. Further, a ~3°C SST decline within the uppermost 100 m of the tropical W-Atlantic during the LGM was taken into consideration (e.g. Rühlemann et al., 1999; Schmidt et al., 2012), in order to simulate water column stability under an extreme, although unrealistic, small density gradient between surface and intermediate ocean.

The modified hydrographic fields were based on observed temperature and salinity fields from the World Ocean Atlas (WOA2013, Boyer et al., 2013) along two sections at 27.5°W (N-S-oriented) and at 12.5°N (W-E-oriented; Fig. S6A). To selectively warm AAIW, we used phosphate concentrations from the same climatological product and defined AAIW by phosphate concentrations above 2 µmol/l, corresponding to 500-1200 m water depth (Fig. S6D) (e.g., Piola & Georgi, 1982; Marchitto & Broecker, 2006; Mawji et al., 2015; Poggemann et al., 2017). We then modified the climatological temperature from WOA2013 using a transition function, which smoothly increases from $\Delta T = 0°C$ at ~0 µmol/l phosphate to $\Delta T = 5°C$ at ~3 µmol/l phosphate (Fig. S6B). To mimic the near-surface cooling during the LGM, we added a cooling profile focused on the upper ocean using an exponential profile with $\Delta T = -3°K$ at the surface and a vertical e-folding scale of 100 m (Fig. S6C). Both modifications were applied at the same time. We then used the modified temperature fields to diagnose static stability as the vertical gradient of locally reference potential density. The resulting stability estimates (Fig. S6E) imply statically unstable conditions in the near-surface ocean, which are due to the cooling profile superimposed on the vertically homogenous hydrography of the mixed layer. These would lead to a limited redistribution of water within the upper 100 m. Above the core of the warmed AAIW, the modified temperature profile yields reduced static stability as is evident from the reduction of the vertical gradient of locally reference potential density, which is, however, never inverted. Consequently, we found that a selective increase of modern-day AAIW temperatures to its assumed deglacial levels by ~5°C is compatible with the modern water mass structure in the Atlantic and in the studied region. All calculations were done in Python 2 using Numpy (Oliphant, 2006), Matplotlib (Hunter, 2007), and the Seawater Toolbox (https://pythonhosted.org/seawater/).

Text S6.

Comparison of standard 400 yr and local 277 yr reservoir age calibration

The age model of Core 235 is based on AMS^{14}C-datings, which were corrected using Calib 7.10 (http://calib.org/calib/) and and the local 277 yr reservoir age (MARINE13), in order to be consistent with Poggemann et al. (2017) and their Core 235 benthic Cd/Ca and δ^{13}C records. The patterns of the reconstructed deglacial $IWT_{Mg/Ca}$ strikingly resemble N-Atlantic AMOC strength reconstructions (Böhm et al. 2015 and references therein) in that marked $IWT_{Mg/Ca}$ rises accompany AMOC perturbations (Fig. S7). When modifying the age model by applying the standard 400 yr reservoir age (IntCal13) to the radiocarbon datings, the apparent temporal lag between $IWT_{Mg/Ca}$ and $^{231}Pa/^{230}Th$ diminishes. The temporal offset across HS1 between the different stratigraphic approaches is ~500 yrs. This stratigraphical vagueness unfortunately hampers any further discussion on temporal phase relationships between deglacial AMOC perturbations, the response of the Southern Ocean, and the possible consequences for the transfer of ocean warmth *via* AAIW.

Text S7.

Intermediate depth seawater Cd records in comparison

Came et al. (2008) were the first to report Cd_w data from the Florida Straits, Core KNR166-2-31JPC (~750 m water depth), which is rather similar to the Valley et al. (2017) Cd_w reconstruction. In contrast to the AAIW Cd_w record from our Core 235 (Poggemann et al., 2017) (Fig. 3, Fig. S4), the Came et al. (2008) record from Florida Straits exhibits overall low Cd_w, with minor Cd_w increases only during the late HS1, the BA and in the Holocene. Times of high Cd_w were interpreted to indicate enhanced northward expansion of AAIW. During the late HS1, instead, when tropical W-Atlantic Cd_w-peaks (our Core 235) point to considerable nutrient injection *via* AAIW due to substantial AMOC re-organisations, the Florida Straits Cd_w data rather exhibit similar Cd_w inreases but at a much lower amplitude. It may be hypothesized that while the AMOC collapsed during HS1, the nutrient enriched AAIW might have penetrated into Florida Straits, although at a lower percentage and highly diluted. More important, other processes might have affected the nutrient budget of Florida Straits. The relatively shallow sill depth of ~740 m in Florida Straits most likely prevented the deep water exchange with the open Atlantic and a strong contribution of nutrient depleted NADW/GNAIW therefore seems unlikely.

Table S1. Calibrated AMS^{14}C dates for sediment core M78/1-222-9 using Calib 7.10 (http://calib.org/calib/) and Marine13 databases using the local 277 yr reservoir age.

Depth (cm)	**Measured Radiocarbon Age (yrs BP)**	**+/- yrs BP**	**Median Age (ka BP)**
3.5	130	30	0.13
113.5	10810	40	12.36
163.5	21020	100	24.87
178.5	22820	120	26.76

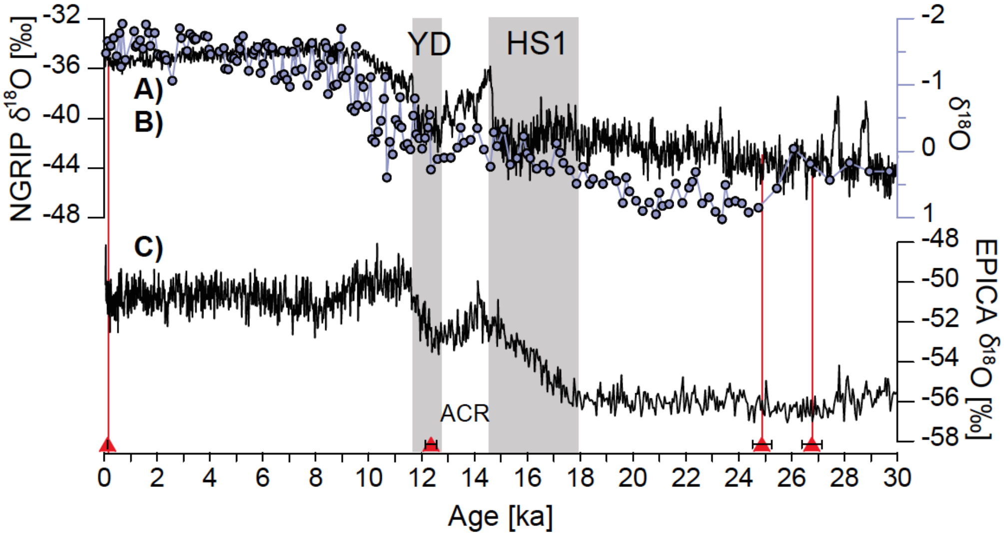

Figure S1. Chronostratigraphy of Core 222, based on radiocarbon (AMS^{14}C) datings (red triangles at x-axis plus error range, and red lines; c.f. Table S1) and linear interpolation in between. The established age model leads to a reasonable visual match between (A) the planktonic stable oxygen isotope record ($\delta^{18}O_{G.ruber}$) of Core 222 (blue) and (B) the Greenland NGRIP ice core δ^{18}O record (NGRIP Dating Group, 2006) reflecting northern hemisphere climate change (black). (C) Antarctica EPICA Dome C δ^{18}O record (Stenni et al., 2006) reflecting the southern hemisphere climate signal (black) for comparison. HS1 = Heinrich Stadial 1; YD = Younger Dryas Stadial; ACR = Antarctic Cold Reversal.

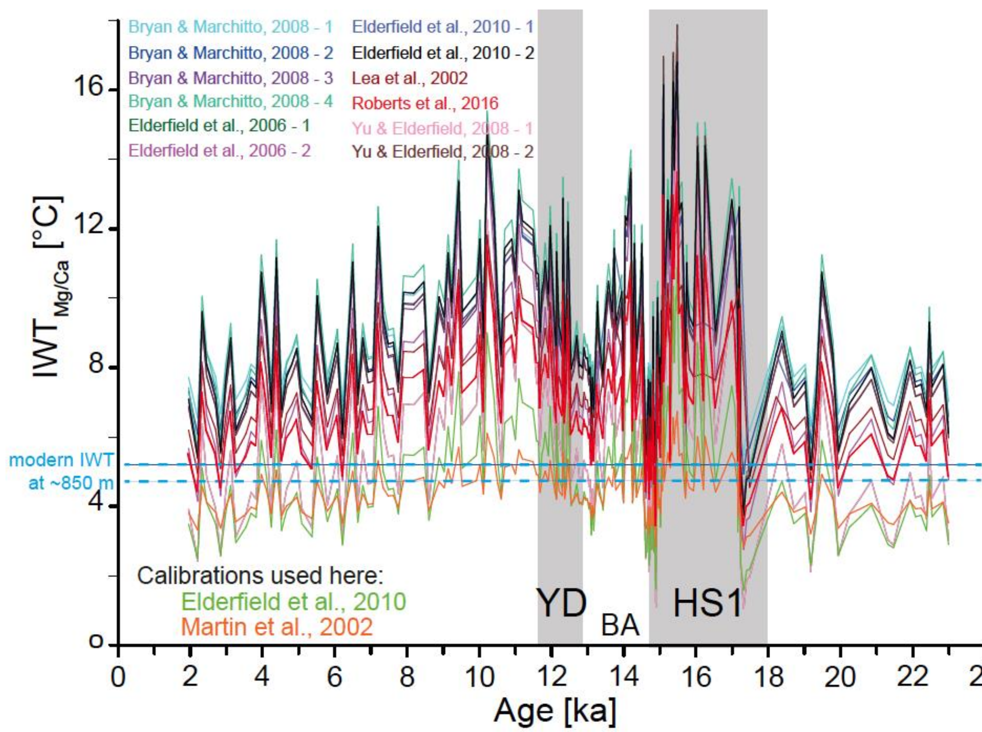

Figure S2. Comparison of linear and exponential temperature calibrations available for *Uvigerina* spp. . Calibrations of Elderfield et al. (2010) and Martin et al. (2002) were considered most reliable (light green and orange). Other calibrations from Lea et al. (2002), Martin et al. (2002), Elderfield et al. (2006), Yu & Elderfield (2008), Brian & Marchitto (2008), and Roberts et al., 2016) were obviated. Dashed blue lines indicate modern IWT at 850 m water depth in the S-Caribbean (from WOA2013; Boyer et al., 2013). HS1 = Heinrich Stadial 1; YD = Younger Dryas Stadial; BA = Bølling-Allerød; ACR = Antarctic Cold Reversal.

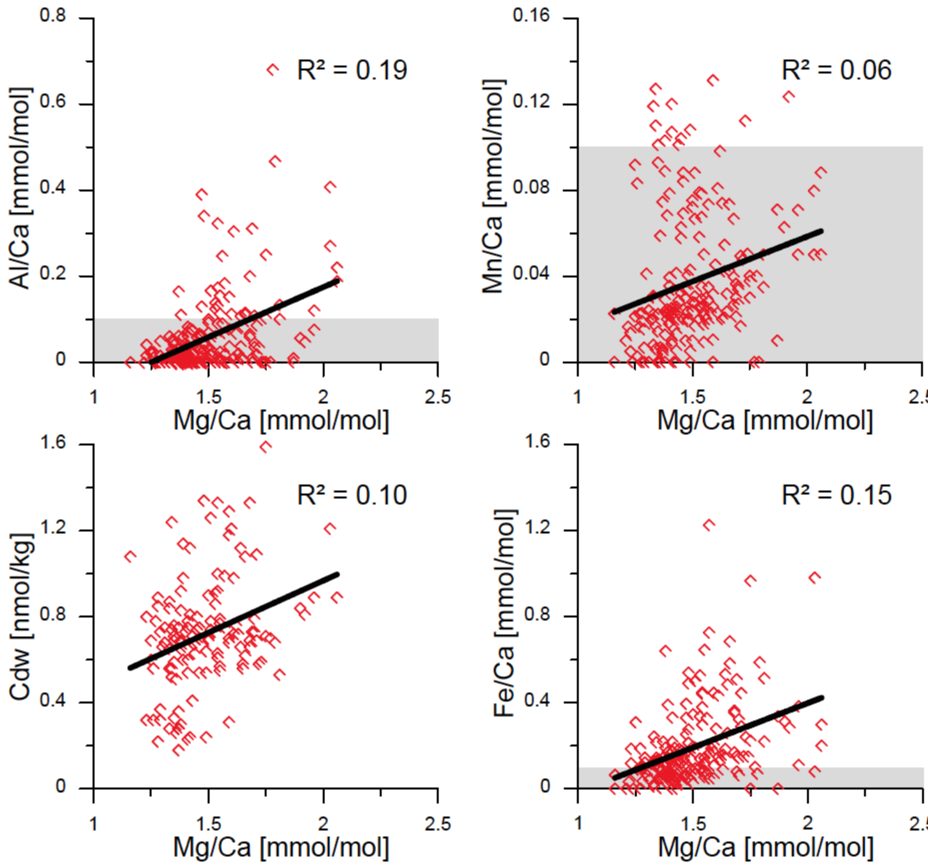

Figure S3. Mg/Ca$_{Uvigerina}$ in relation to contaminant phases Al/Ca (top left), Mn/Ca (top right), and Fe/Ca (bottom right) from the same foraminiferal samples. Correlation coefficients R^2 point to overall low correlations. Contaminant elemental ratios mostly remain below the threshold values given by Barker et al. (2003) and Them et al. (2015) indicative of sample contamination (0.1 mmol/mol; gray shading). At bottom left: Mg/Ca$_{Uvigerina}$ *vs.* seawater Cd values (Cd_w) calculated from foraminiferal Cd/Ca$_{Uvigerina}$ (Poggemann et al., 2017) from the same samples.

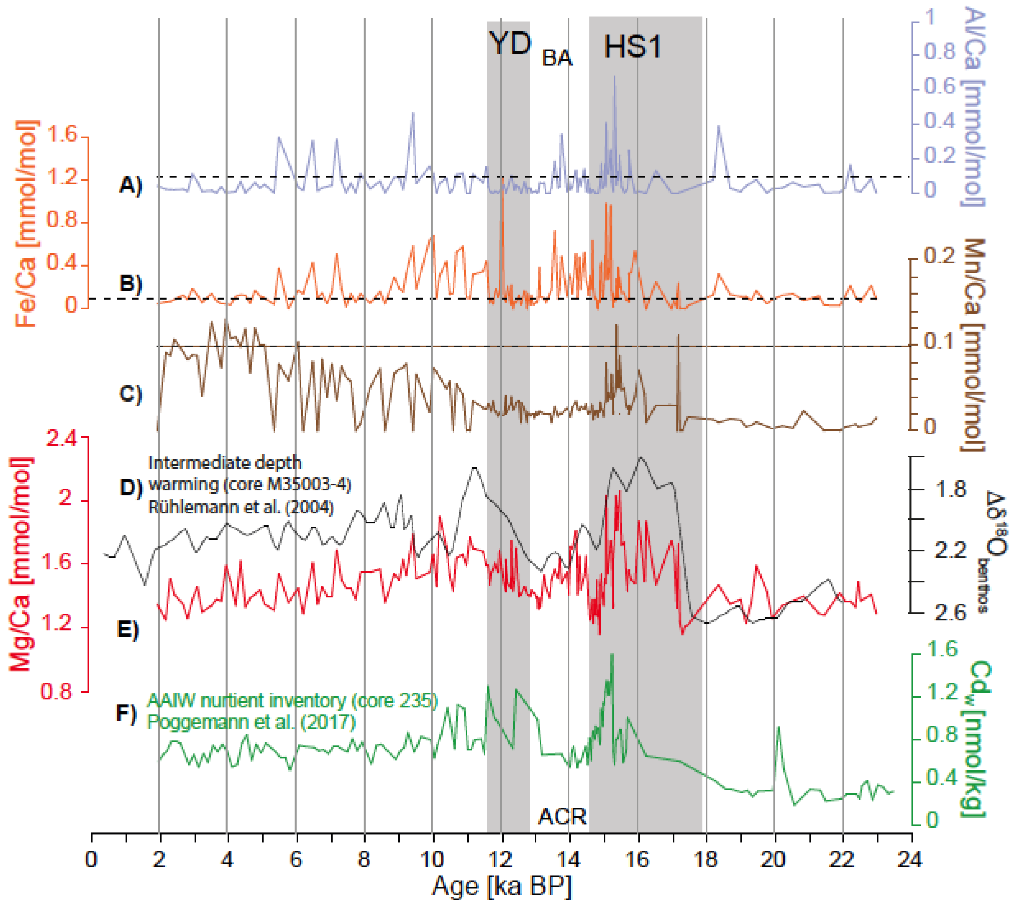

Figure S4. Downcore Mg/Ca*Uvigerina* of Core 235 (E) in comparison to contaminant element ratios Al/Ca (A), Fe/Ca (B), and Mn/Ca (C) from the same samples. Correlation coefficients are given in Fig. S3. Threshold values provided by Barker et al. (2003) and Them et al. (2015) indicative of sample contamination (0.1 mmol/mol) are marked by dashed horizontal lines. Note that these threshold values are likely not valid for the sediment core studied here. (D) The intermediate water temperature estimation (Core 35003-4 from Tobago Basin, 1299 m water depth) based on ice-volume corrected benthic $\delta^{18}O$ values (Rühlemann et al., 2004) corresponds closely to the Mg/Ca*Uvigerina* record of Core 235, and hence to $IWT_{Mg/Ca}$. (E) shows seawater Cd values (Cd_w) of Core 235 derived from Cd/Ca*Uvigerina* revealing that deglacial nutrient and ocean temperature evolution within AAIW had different timing.

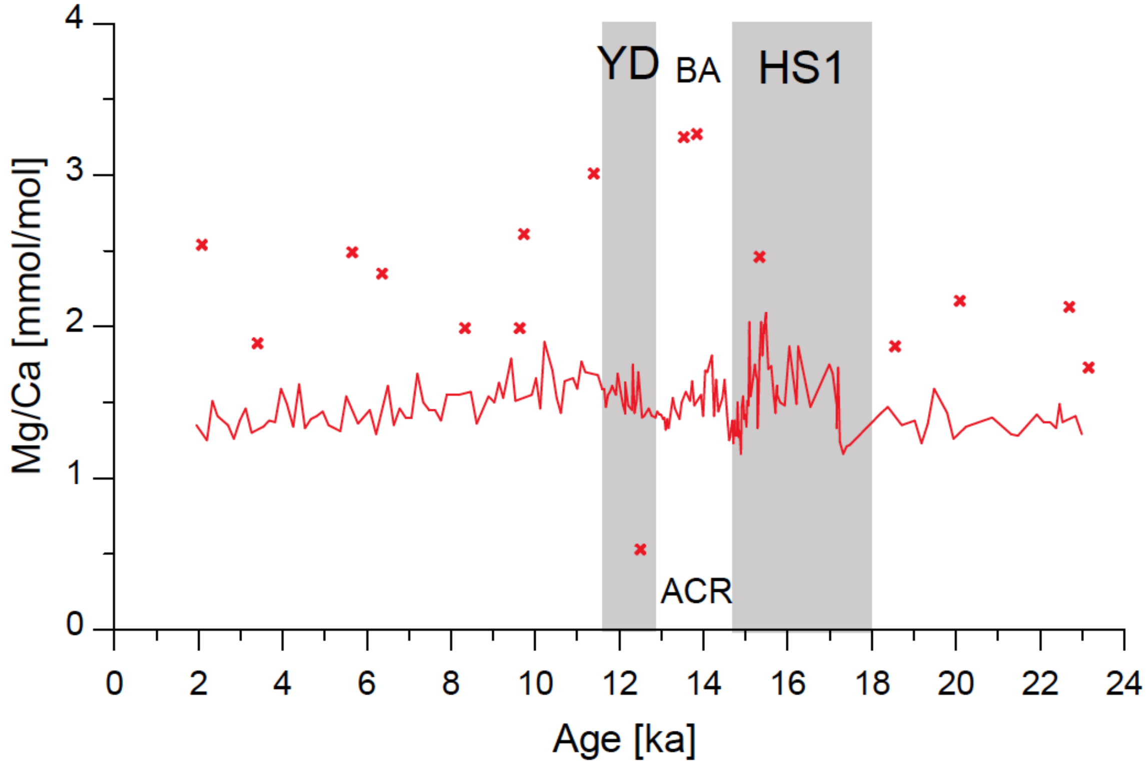

Figure S5. Mg/Ca$_{Uvigerina}$ data for Core 235. Overall, 16 data points are unrealistically high (or low). By applying the Grubbs test (Grubbs, 1950; 1969), these data points were defined as outliers and excluded from interpretation of the dataset (crosses). HS1 = Heinrich Stadial 1; YD = Younger Dryas Stadial; BA = Bølling-Allerød; ACR = Antarctic Cold Reversal.

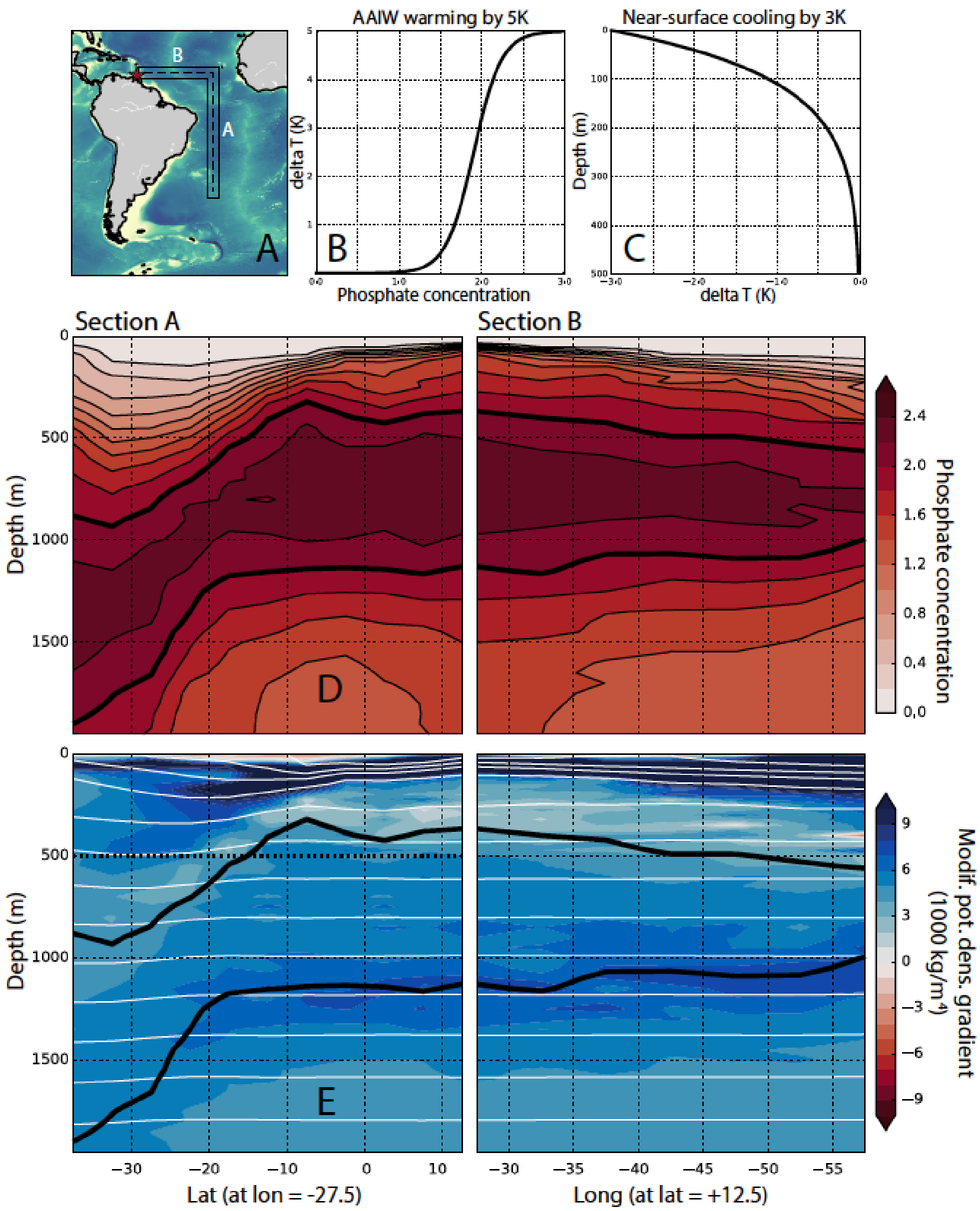

Figure S6. Static stability test calculations at modulated IWT and SST conditions and resulting vertical density gradient. **A**) Calculations were done along two sections A and B with the area covered by the climatological grid; position of Core 235 indicated by the star. **B**) The IWT increase was moderated by phosphate concentration. Temperature was smoothly increased by up to 5K for phosphate concentrations above 3 µmol/l. **C**) Decreased sea surface temperature pattern as postulated for the LGM. **D**) Modern phosphate concentration along sections A and B (WOA2013; Boyer et al., 2013). Thick contour lines indicate a phosphate concentration of 2 µmol/l and hence, enclose the regions where temperatures were increased. **E**) Vertical gradient of locally referenced potential density (1000 kg/m^4) from the modified temperature fields along sections A and B. Negative values indicating static instability is only found in the very upper part of the water colum where the imposed exponential cooling would be replaced by a homogeneous vertical profile within the surface mixed layer. Throughout the rest of the water column, conditions remain stable (positive gradients). Hence, warmed AAIW would not violate the modern-day stratification. All calculations were done in Python 2 using Numpy (Oliphant, 2006), Matplotlib (Hunter, (2007), and the Seawater Toolbox (https://pythonhosted.org/seawater/).

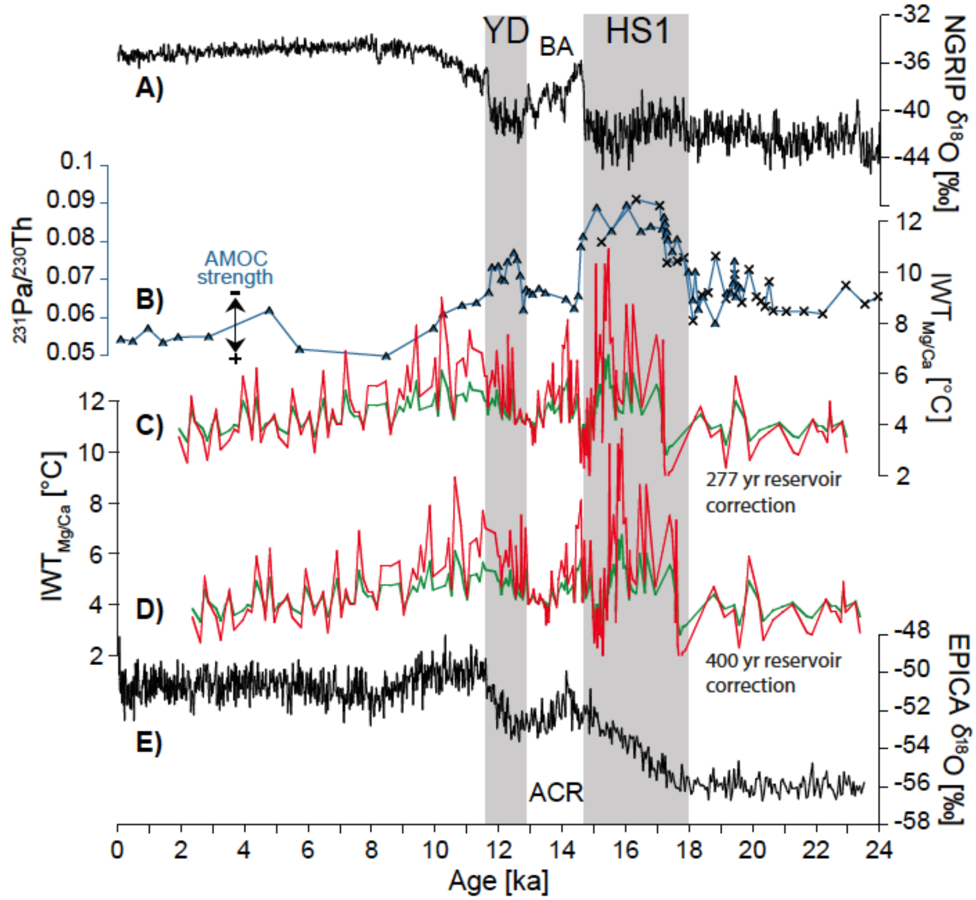

Figure S7. Comparison of different reservoir age assumptions applied in the age model of Core 235. (A) Greenland NGRIP ice core $\delta^{18}O$ record (NGRIP Dating Group, 2006) reflecting northern hemisphere climate change (black) for comparison. (B) $^{231}Pa/^{230}Th$ data (blue) of N-Atlantic ODP Site 1063 (Böhm et al., 2015 and references therein) reflecting N-Atlantic overturning strength with high values pointing to weakened AMOC. (C) $IWT_{Mg/Ca}$ records of Core 235 (red record = $Mg/Ca_{\mathit{Uvigerina}}$ calibrated according to Elderfield et al., 2010; green record = $Mg/Ca_{\mathit{Uvigerina}}$ calibrated according to Martin et al., 2002) with an age model corrected using Calib 7.10 and the local 277 yr reservoir age (MARINE13) similar to Poggemann et al. (2017). (D) the same $IW_{Mg/Ca}$ records as in (C) with an age model corrected using Calib 7.10 and the standard 400 yr reservoir age (IntCal13). (E) Antarctica EPICA Dome C $\delta^{18}O$ record (Stenni et al., 2006) reflecting the southern hemisphere climate signal (black) for comparison. HS1 = Heinrich Stadial 1; YD = Younger Dryas Stadial; BA = Bølling-Allerød; ACR = Antarctic Cold Reversal.

Data Set S1. Geochemical data *vs.* core depth and age. 1.) Foraminiferal Mg/Ca, Al/Ca, Mn/Ca, and Fe/Ca ratios of *Uvigerina* spp. from Core M78/1-235-1 (11°36.53'N, 60°57.86'W; 852 m water depth). Outliers are indicated. Intermediate water temperatures ($IWT_{Mg/Ca}$) were calculated from Mg/Ca using the calibrations of Martin et al. (2002) and Elderfield et al. (2010). 2.) The εNd signatures of uncleaned mixed planktonic foraminifera from Core M78/1-222-9 (12°1.49'N, 64°28.50'W, 1018 m water depth). Data uploaded to AGU's journal submission site.